Electrochemical Properties of Oxygenated Cup-Stacked Carbon Nanofiber-Modified Electrodes

Journal:	*Physical Chemistry Chemical Physics*
Manuscript ID:	CP-ART-03-2014-001278.R1
Article Type:	Paper
Date Submitted by the Author:	18-Apr-2014
Complete List of Authors:	Ko, Seongjae; University of Tokyo, Institute of Industrial Science Tatsuma, Tetsu; University of Tokyo, Institute of Industrial Science Sakoda, Akiyoshi; University of Tokyo, Institute of Industrial Science Sakai, Yasuyuki; University of Tokyo, Institute of Industrial Science Komori, Kikuo; University of Tokyo, Institute of Industrial Science

PCCP

RSCPublishing

ARTICLE

Electrochemical Properties of Oxygenated Cup-Stacked Carbon Nanofiber-Modified Electrodes

Cite this: DOI: 10.1039/x0xx00000x

Seongjae Ko, Tetsu Tatsuma, Akiyoshi Sakoda, Yasuyuki Sakai and Kikuo Komori*

Received 00th January 2012,
Accepted 00th January 2012

DOI: 10.1039/x0xx00000x

www.rsc.org/

Oxygenated cup-stacked carbon nanofibers (CSCNFs), the surface of which provide highly ordered graphene edges and oxygen-containing functional groups, were investigated as electrode materials by using typical redox species in electrochemistry, $Fe^{2+/3+}$, $[Fe(CN)_6]^{3-/4-}$, and dopamine. The electron transfer rates for those redox species at oxygenated CSCNF electrodes were higher than those at edge-oriented pyrolytic graphite and glassy carbon electrodes. In addition, the oxygen-containing functional groups also contributed to the electron transfer kinetics at the oxygenated CSCNF surface. The electron transfer rate of $Fe^{2+/3+}$ was accelerated and that of $[Fe(CN)_6]^{3-/4-}$ was decelerated by the oxygen-containing groups, due mainly to the electrostatic attraction and repulsion, respectively. The electrochemical reaction selectivities at the oxygenated CSCNF surface were tunable by controlling the nanofiber amount and the oxygen/carbon atomic ratio at the nanofiber surface. Thus, the oxygenated CSCNFs would be useful electrode materials for energy-conversion, biosensing, and other electrochemical devices.

Introduction

Study of edge plane sites of graphene has attracted a great attention, because electronic, chemical, and magnetic properties of graphene are strongly influenced by graphene edges.[1, 2] In the area of electrochemistry, it has been known that the electron transfer reaction with redox species is accelerated at the edge plane sites compared with the basal plane site of graphene.[3-7] Additionally, it has also been reported that the peripheral edge of carbon nanotubes (CNTs) with a cylindrical structure plays an important role in fast electron transfer reactions with redox species.[8-11] These phenomena are considered to be akin to edge-oriented and basal-plane pyrolytic graphite (EOPG and BPPG) electrodes, because a heterogeneous electron transfer reaction at the former electrode is generally faster than that at the latter one.[12] Recently, nanofibers with stacked graphene, such as platelet carbon nanofibers (PCNFs), cup-stacked carbon nanofibers (CSCNFs), and herringbone carbon nanofibers (HCNFs), are focused as a new conducting material, because such carbon nanofibers provide a high density of exposed and reactive edges at fiber surfaces compared with CNTs. Hence, the study of the edge plane sites at the nanofiber surface becomes increasingly important.

The edges are also easily oxidized so that oxygen-containing functional groups are introduced. The oxygen-containing groups would afford selectivity to the nanofibers based on interaction between the groups and redox species. In addition, sufficiently oxygenated nanofibers with stacked graphene can be dispersed in a solvent such as water.[13, 14] The dispersed nanofibers allow easy coating and patterning of carbon nanofiber films. Those films consisting of nanofibers with stacked graphene expose a high density of graphene edges without control of the fiber orientation, whereas CNTs, which have graphene edges only at the ends of nanotube, must be vertically oriented to expose graphene edges. In addition, in the case of CNTs, sufficient oxygenation causes degradation of the two-dimensional network of sp^2 carbon.

Recently, we have successfully synthesized CSCNFs by a chemical vapor deposition (CVD) method based on the catalytic pyrolysis of poly(ethylene glycol) (PEG).[15, 16] Inner and outer diameters of the resultant CSCNFs were about 20 and 30 nm, respectively. Its length was several micrometers. The graphene layers were inclined at an angle of 5-25 degrees with respect to the fiber axis. We previously confirmed that the CSCNFs worked as an electric nanowire and enzyme support.[17] In addition, CSCNFs have so far been used for electrochemical solar cells[18] and electrochemical capacitors.[19] However, electrochemical properties for oxygenated CSCNFs, in particular their reaction selectivity have not yet been well investigated. In the present study, we report the electrochemical properties of oxygenated CSCNFs. We modified glassy carbon (GC) electrodes with thermally oxidized CSCNFs and examined their electrochemical responses to three redox species, iron(II) chloride ($FeCl_2$),

potassium ferricyanide ($K_3[Fe(CN)_6]$), and dopamine, which have commonly been used for electrochemical characterization of carbon electrodes. We controlled the amount of CSCNFs and the degree of oxygenation at their edge plane sites to study the electron transfer kinetics for those redox species.

Experimental

Preparation of CSCNFs

CSCNFs were prepared according to our previous reports.[15, 16] An aqueous solution containing 7.5 mM $NiCl_2$ and 8.0 M PEG (Mw = 8 000, Wako Pure Chemicals, Japan) was stirred for 30 min at 60 ˚C and then coated on a silicon wafer (150 mg cm^{-2}) uniformly. The silicon wafer was placed on a hot plate at 60 ˚C for 1 h, followed by cooling at room temperature for 2 h. The PEG-nickel membrane-coated silicon wafer was placed in a quartz pipe (7.5 cm in diameter and 85 cm long) and heated to 750 ˚C in an electric oven at a heating rate of 15 ˚C min^{-1} under an argon atmosphere. The temperature was maintained at 400, 500, and 750 ˚C for 1 h each to obtain CSCNFs.

Oxygenation and Deoxygenation of CSCNFs

The as-grown CSCNFs in the quartz pipe were thermally treated at 540 ˚C for 1 h in the electric oven under the atmosphere to give oxygenated CSCNFs (ox-CSCNFs) with oxygen-containing functional groups. The heating temperature was decided on the basis of the thermogravimetric analysis (TGA) curve of the as-grown CSCNFs (Figure 1A); its thermo-oxidative degradation begins at 500 ˚C and its weight decreases nearly 15% at 540 ˚C. We could not obtain a sufficient amount of ox-CSCNFs at temperatures above 580 ˚C due to extensive thermo-oxidative degradation. The ox-CSCNFs were further heated at 400 ˚C for 10 min or 600 ˚C for 30 min under a nitrogen atmosphere to give partially deoxygenated CSCNFs (deox1- or deox2-CSCNFs, respectively); the surface coverage of oxygen-containing functional groups was controlled by thermal desorption.

Atomic oxygen/carbon (O/C) ratios of the CSCNF samples were examined by XPS (PHI Quantera SXM^{TM}, Ulvac-Phi Inc., Japan). The structure of CSCNFs were analyzed using a Raman spectrometer (T-64000, Horiba Ltd., Japan) and a temperature programmed desorption (TPD) system consisting of an electric tubular furnace (ARF-40K, Asahirika Seisakusho) and gas analyzers for carbon monoxide (HT-1210N, Hodaka Co., Ltd.) and carbon dioxide (ZFP5YA31, Fuji Electric Co., Ltd.). Zeta potential was determined by a Zetasizer Nano ZS (Malvern Instruments Ltd, UK).

Preparation of Electrodes Modified with CSCNFs

The oxygenated and deoxygenated CSCNFs were dispersed in *N*,*N*-dimethylformamide (DMF) at 0.1 mg mL^{-1}. CSCNF-modified GC electrodes (ca. 0.28 cm^2) were prepared by casting 10–100 μL of the suspension. After evaporation of DMF, the electrodes were immersed in a 1.0 M H_2SO_4 aqueous solution for 30 min to remove the nickel catalyst, followed by thoroughly rinsing with distilled water.

Electrochemical measurements were performed in a 1.0 M H_2SO_4 aqueous solution containing 1.0 mM $FeCl_2$ or a 0.067 M phosphate buffer solution (pH 6.4) containing 1.0 mM $K_3[Fe(CN)_6]$ or 1.0 mM dopamine with a potentiostat Versa STAT (Princeton Applied Research, USA). A Ag|AgCl|KCl sat. and a coiled platinum wire were used as reference and counter electrodes, respectively.

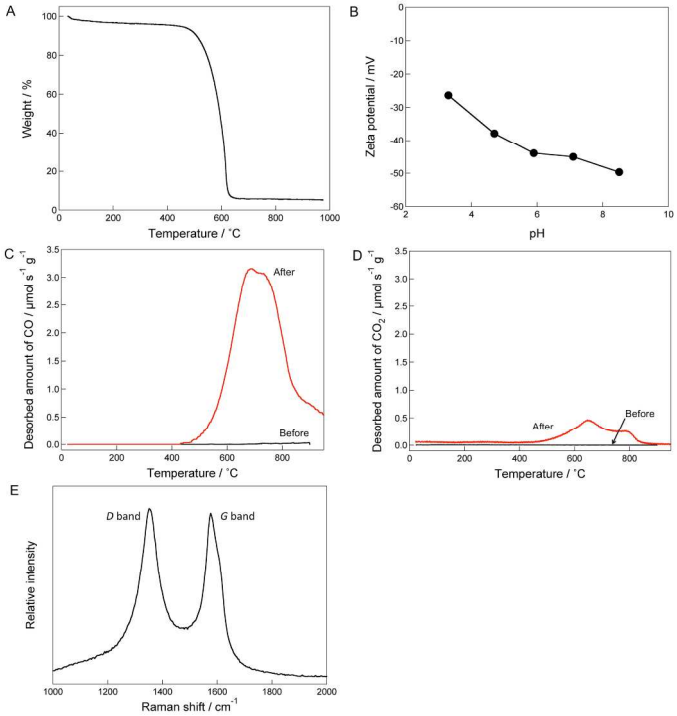

Figure 1. (A) TGA curve of as-grown CSCNFs. (B) Dependence of zeta potential for ox-CSCNFs on pH. (C) CO and (D) CO_2 TPD spectra of as-grown CSCNFs and ox-CSCNFs. (E) Raman spectra of ox-CSCNFs.

Results and Discussion

Oxygenation and Deoxygenation of CSCNFs

Although the as-grown CSCNFs could not be suspended in DMF and water, those were dispersible after the thermal treatment in air at 540 ˚C. This suggests that oxygen-containing functional groups are introduced to CSCNFs, likely at the edge plane sites. Actually, the atomic O/C ratio at the CSCNF surface determined by XPS was increased from ~3% to 32.3 ± 1.5% (mean ± standard error, n = 3) after the treatment. We also measured zeta potential of ox-CSCNFs. The surfaces of ox-CSCNFs were negatively charged in the entire pH range examined here (Figure 1B). This result might be based on not only delocalized π electrons at the CSCNF surface but also oxygen-containing functional groups at the edge plane sites.

We further analyzed oxygen-containing functional groups on ox-CSCNFs by a TPD method. If oxygen-containing functional groups, such as carboxyl and phenol groups, are present on the CSCNF surface, CO and CO_2 should be released from the surface by thermal desorption during thermal

treatment under an inert gas.[20-23] Figure 1C and D shows TPD charts of CSCNFs before and after the thermal treatment. The amounts of CO and CO_2 gases released from the as-grown CSCNFs were negligibly small. In contrast, significant amounts of the gases were desorbed from ox-CSCNFs. The desorption of CO is attributed to anhydride (> 400 ˚C), phenol (> 600 ˚C), ether, carbonyl, and quinone (700 ˚C) groups.[20-23] Meanwhile, CO_2 released above 400 ˚C is ascribed to lactone groups and/or anhydrides.[20-23] It is, however, difficult to determine the amount of each oxygen-containing functional group precisely from the TPD results.

We also examined ox-CSCNFs by Raman spectroscopy, which is frequently used for characterization of carbon materials. As Figure 1E shows, ox-CSCNFs exhibit Raman peaks at approximately 1350 and 1590 cm^{-1}. It is known that carbon atoms in a well-ordered graphene structure exhibit a *G*-band signal at about 1590 cm^{-1}, whereas carbon atoms adjacent to a defect or a graphene edge exhibit a *D*-band signal at about 1350 cm^{-1}.[24]

The thermal treatment of ox-CSCNFs under N_2 decreased the atomic O/C ratio to 15.8 ± 1.1 and 7.9 ± 0.8% for deox1-CSCNFs (400 ˚C for 10 min) and deox2-CSCNFs (600 ˚C for 30 min), respectively. It is therefore obvious that ox-CSCNFs were deoxygenated partially by the treatment.

Electrochemical Behavior of $Fe^{2+/3+}$

We next examined electrochemical behavior of the three selected redox species, namely Fe^{2+}, $[Fe(CN)_6]^{3-}$, and dopamine, at EOPG, GC, and the ox-CSCNF-modified GC electrodes. At first, we used $Fe^{2+/3+}$, the electron transfer kinetics of which is known to be strongly sensitive to the oxygen containing functional groups at the carbon surface.[25, 26]

Figure 2A shows cyclic voltammograms (CVs) recorded in an air saturated 1.0 M H_2SO_4 aqueous solution containing 1.0 mM $FeCl_2$, where the scan rate was 50 mV s^{-1}. The peak-to-peak potential separation (ΔE_P) at the EOPG electrode (438 mV) was smaller than that at GC (669 mV) probably due to the edge plane sites of EOPG, where oxygen containing functional groups should essentially be absent because the EOPG electrode was used soon after polishing its surface.[27] The ΔE_P value for the ox-CSCNF electrode (1.1×10^{-5} g cm^{-2}) (156 mV) was even smaller than those at the GC and EOPG electrodes. This reflects that the electron transfer is faster at the ox-CSCNF electrode, and the fast kinetics may be attributed to the edge plane sites, which may facilitate the electron transfer, and/or the oxygen-containing groups, which may have chemical and/or electrostatic interaction with $Fe^{2+/3+}$, which usually undergo inner-sphere redox reactions.[28] Based on the method developed by Nicholson,[29] we determined an apparent heterogeneous electron transfer rate constant, k^0_{app}, based on projected electrode area. Assuming that $\alpha = 0.5$ and diffusion coefficient $D = 5.1 \times 10^{-6}$ cm^2 s^{-1},[30] the k^0_{app} value at the ox-CSCNF electrode was determined from the dependence of ΔE_P on the scan rate to be $2.3 \pm 0.5 \times 10^{-3}$ cm s^{-1} ($n = 3$). This value was at least one order of magnitude larger than those for EOPG and GC electrodes (< 10^{-4} cm s^{-1}). In addition, the k^0_{app} value was three orders of magnitude larger than that at graphene oxide electrodes reported previously.[31] This means that unlike the graphene oxide, oxygenated CSCNFs maintained the sp^2 carbon network without serious defects.

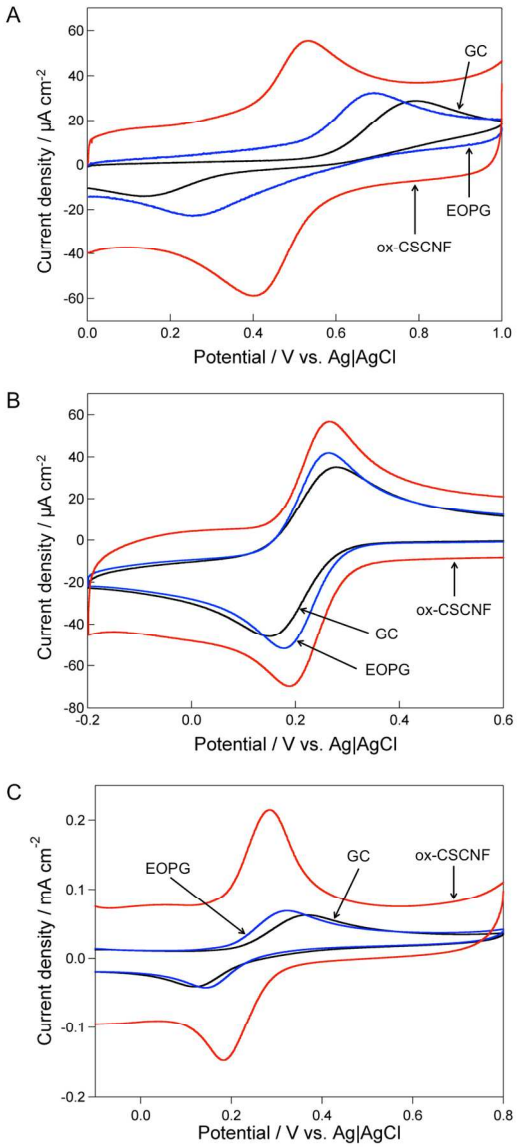

Figure 2. Cyclic voltammograms of (A) 1.0 mM $FeCl_2$ in a 1.0 M H_2SO_4 aqueous solution, (B) 1.0 mM $K_3[Fe(CN)_6]$ in a 0.067 M phosphate buffer (pH 6.4), and (C) 1.0 mM dopamine in a 0.067 M phosphate buffer (pH 6.4) on EOPG, GC, and ox-CSCNF electrodes. The amount of ox-CSCNFs at the electrode surface is about 1.1×10^{-5} g cm^{-2}. Scan rate is (A) 50 and (B and C) 100 mV s^{-1}.

We next controlled the amount of ox-CSCNFs on the GC electrode surface and investigated its effect on the electron transfer rate. The ΔE_P values decreased and the k^0_{app} value increased as the amount of ox-CSCNFs increased, as shown in Figure 3. To confirm the possible contribution of the oxygen-containing functional groups to the enhancement of the electrode kinetics, we replaced ox-CSCNFs with deox1- or deox2-CSCNFs to control the O/C ratio at the fiber surface. As shown in Figure 4, the k^0_{app} value increased as the O/C ratio increased, whereas the amount of nanofibers deposited on the

electrode surface was constant, about 1.1×10^{-5} g cm^{-2}. These results clearly indicate that the oxygen-containing groups mainly contribute to the increase in the electron transfer rate for $Fe^{2+/3+}$. Thus, deposition of a large amount of CSCNFs with a high O/C ratio on the electrode surface would allow further acceleration of the $Fe^{2+/3+}$ redox reactions.

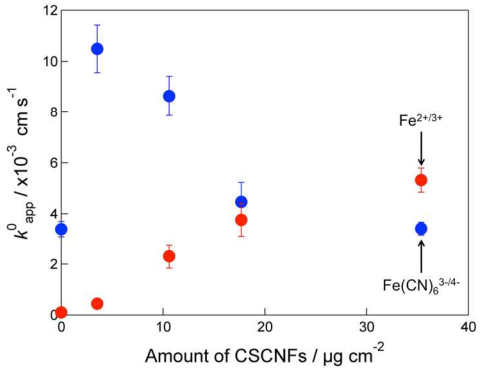

Figure 3. Relationship between the amount of ox-CSCNFs on the electrode surface.

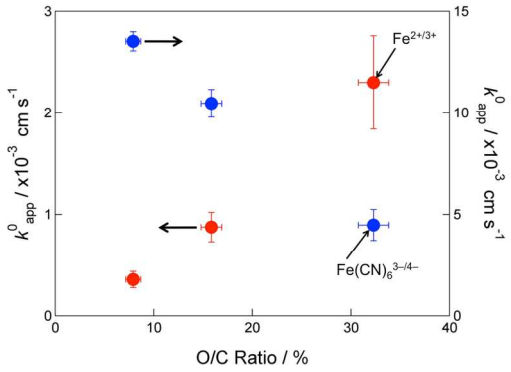

Figure 4. Relationship between the k^0_{app} value of $Fe^{2+/3+}$ and $[Fe(CN)_6]^{3-/4-}$ and the O/C atomic ratio of the CSCNF surface. The amount of ox-CSCNFs at the electrode surface is about 1.8×10^{-5} g cm^{-2}.

Electrochemical Behavior of $[Fe(CN)_6]^{3-/4-}$

We next examined the $[Fe(CN)_6]^{3-/4-}$ redox couple. The redox behavior of $[Fe(CN)_6]^{3-/4-}$ has been extensively studied in electrochemistry and is known to be outer-sphere process in general.[28] Figure 2B shows CVs recorded in a 0.067 M phosphate buffer solution (pH 6.4) containing 1.0 mM $[Fe(CN)_6]^{3-/4-}$, where the scan rate was 100 mV s^{-1}. Again, the ΔE_P value at the ox-CSCNF electrode (1.1×10^{-5} g cm^{-2}) (79 mV) was smaller than those at the EOPG (89 mV) and GC (121 mV) electrodes. Here, the k^0_{app} values were about $8.6 \pm 0.8 \times 10^{-3}$, $5.8 \pm 0.5 \times 10^{-3}$, and $3.4 \pm 0.3 \times 10^{-3}$ cm s^{-1} for ox-CSCNF, EOPG, and GC electrodes, respectively, on the assumption that $\alpha = 0.5$ and diffusion coefficient $D = 7.6 \times 10^{-6}$ cm^2 s^{-1}.[32]

The dependence of the k^0_{app} value on the amount of ox-CSCNFs was also examined. Interestingly, the k^0_{app} value increased and then decreased as the amount increased (Figure 3). This suggests that at least two different factors control the electron transfer rate; the graphene edges positively and the oxygen-containing groups negatively contribute to the electron transfer most likely. Since $[Fe(CN)_6]^{3-/4-}$ undergoes outer-sphere electron transfer, the oxygen-containing groups do not exhibit a catalytic effect. Rather, the electrostatic repulsion between the negatively charged oxygen-containing groups and $[Fe(CN)_6]^{3-/4-}$ decelerates the electron transfer. In fact, we found that the k^0_{app} value decreased as the O/C ratio increased, as shown in Figure 4 (nanofiber coverage is 1.8×10^{-5} g cm^{-2}). This is reasonable because the electron transfer of $[Fe(CN)_6]^{3-/4-}$ is known to be decelerated at oxygenated EOPG,[27] diamond[26] and graphene oxide[31, 33] electrodes due to the electrostatic repulsion. Considering our finding here, use of a small amount of CSCNF with the lowest possible O/C ratio may allow for further acceleration of the $[Fe(CN)_6]^{3-/4-}$ redox reactions.

Electrochemical Behavior of Dopamine

We further investigated electrochemistry of an organic redox species, dopamine. It is known that dopamine is one of the important neurotransmitters and its electron transfer is affected by the surface morphology of electrodes.[5] Figure 2C shows CVs in a 0.067 M phosphate buffer solution (pH 6.4) containing 1 mM dopamine, where the scan rate is 100 mV s^{-1}. The ΔE_P values were 176, 243, and 110 mV at the EOPG, GC, and ox-CSCNF (1.1×10^{-5} g cm^{-2}) electrodes. Here we examined adsorption of dopamine to the ox-CSCNF surface due to π-π interaction or hydrogen bonding, by changing the scan rate. However, the anodic and cathodic peak currents were nearly proportional to the square root of the scan rate, as was the case for the other redox species examined, so that dopamine hardly adsorbed at the CSCNF surface. Although it is difficult to determine the k^0_{app} values by the Nicholson method, because dopamine oxidation is a multistep process,[34] the k^0_{app} value at the ox-CSCNF electrode should be larger than those at the GC and EOPG electrodes, because the ΔE_P value at the former electrode was much smaller than those at the latter electrodes, as mentioned above.

The ΔE_P value was almost independent of the amount of nanofiber and the O/C ratio. Since the pK_a values of dopamine are 8.89 (first phenolic hydroxy group), 10.4 (amino group), and 13.1 (second phenolic hydroxy group),[35] dopamine molecule should have only one positive charge at the amino group at pH 6.4. The poor dependence of the oxidation kinetics of dopamine on the amount of the oxygen-containing groups at the nanofiber surface may be explained in terms of its weaker electrostatic interaction in comparison with $Fe^{2+/3+}$, which have more positive charges.

Conclusion

The electrochemical properties of oxygenated CSCNFs were investigated to explore their applicability as electrode materials. The electron transfer rate for all redox species used here was accelerated by the oxygenated CSCNFs. In addition, the kinetics of $Fe^{2+/3+}$ and $[Fe(CN)_6]^{3-/4-}$ is tunable by changing the

amount of oxygenated CSCNFs and the O/C ratio at the nanofiber surface. Those factors are therefore subject to optimization in different applications, such as energy-conversion, biosensing, and other electrochemical devices.

Acknowledgement

We are very grateful to Dr. Y. Takahashi and Dr. M. Kamiko for their help with the XPS measurements. This work was partially supported by an International Cooperative Program of the Japan Science and Technology Agency (JST, Japan).

Notes and references

Institute of Industrial Science, University of Tokyo, Komaba, Meguro-ku, Tokyo 153-8505, Japan. E-mail: kkomori@iis.u-tokyo.ac.jp

† Footnotes should appear here. These might include comments relevant to but not central to the matter under discussion, limited experimental and spectral data, and crystallographic data.
Electronic Supplementary Information (ESI) available: [details of any supplementary information available should be included here]. See DOI: 10.1039/b000000x/

1 X. Jia, J. Campos-Delgado, M. Terrones, V. Meunier and M. S. Dresselhaus, *Nanoscale*, 2011, **3**, 86-95.
2 X. Zhang, J. Xin and F. Ding, *Nanoscale*, 2013, **5**, 2556-2569.
3 A. Ambrosi, T. Sasaki and M. Pumera, *Chem. Asian J.*, 2010, **5**, 266-271.
4 D. A. C. Brownson, M. J. Munro, D. K. Kampouris and C. E. Banks, *RSC Adv.*, 2011, **1**, 978-988.
5 A. Ambrosi, A. Bonanni and M. Pumera, *Nanoscale*, 2011, **3**, 2256-2260.
6 W. Yuan, Y. Zhou, Y. Li, C. Li, H. Peng, J. Zhang, Z. Liu, L. Dai and G. Shi, *Sci. Rep.*, 2013, **3**, 2248.
7 G. P. Keeley, N. McEvoy, H. Nolan, M. Holzinger, S. Cosnier and G. S. Duesberg, *Chem. Mater.*, 2014, **26**, 1807-1812.
8 J. Li, A. Cassell, L. Delzeit, J. Han and M. Meyyappan, *J. Phys. Chem. B*, 2002, **106**, 9299-9305.
9 J. J. Gooding, R. Wibowo, J. Liu, W. Yang, D. Losic, S. Orbons, F. J. Mearns, J. G. Shapter and D. B. Hibbert, *J. Am. Chem. Soc.*, 2003, **125**, 9006–9007.
10 F. Patolsky, Y. Weizmann and I. Willner, *Angew. Chem., Int. Ed.*, 2004, **43**, 2113–2117.
11 A. Chou, T. Böcking, N. K. Singh and J. J. Gooding, *Chem. Commun.*, 2005, 842-844.
12 C. E. Banks, T. J. Davies, G. G. Wildgooses and R. G. Compton, *Chem. Commun.*, 2005, 829-841.
13 L. Li and C. M. Lukehart, *Chem. Mater.*, 2006, **18**, 94-99.
14 L. Wu, X. Zhang and H. Ju, *Analyst*, 2007, **132**, 406-408.
15 Y. Takahashi, H. Fujita, W.-H. Lin, Y.-Y. Li, T. Fujii and A. Sakoda, *Adsorption*, 2010, **16**, 57-68.
16 S. Ko, Y. Takahashi, A. Sakoda, Y. Sakai and K. Komori, *Langmuir*, 2012, **28**, 8760-8766.
17 S. Ko, Y. Takahashi, H. Fujita, T. Tatsuma, A. Sakoda and K. Komori, *RSC Adv.* 2012, **2**, 1444-1449.
18 T. Hasobe, S. Fukuzumi and P. V. Kamat, *Angew. Chem. Int. Ed.*, 2006, **45**, 755-759.
19 I. Y. Jang, H. Ogata, K. C. Park, S. H. Lee, J. S. Park, Y. C. Jung, Y. J. Kim, Y. A. Kim and M. Endo, *J. Phys. Chem. Lett.*, 2010, **1**, 2099-2103.
20 A. Dandekar, R. T. K. Baker and M. A. Vannice, Carbon, 1998, **36**, 1821-1831.
21 J. L. Figueiredo, M. F. R. Pereira, M. M. A. Freitas and J. J. M. Órfão, *Carbon*, 1999, **37**, 1379-1389.
22 J.-H. Zhou, Z.-J. Sui, J. Zhu, P. Li, D. Chen, Y.-C. Dai and W.-K. Yuan, *Carbon*, 2007, **45**, 785-796.
23 S. Kundu, Y. Wang, W. Xia and M. Muhler, *J. Phys. Chem. C*, 2008, **112**, 16869-16878.
24 M. S. Dresselhaus, A. Jorio, M. Hoffman, G. Dresselhaus, R. Saito, *Nano Lett.*, 2010, **10**, 751−758.
25 P. Chen, M. A. Fryling and R. L. McCreery, *Anal. Chem.*, **1995**, 67, 3115-3122.
26 I. Yagi, H. Notsu, T. Kondo, D. A. Tryk and A. Fujishima, *J. Electroanal. Chem.*, 1999, **473**, 173-178.
27 X. Ji, C. E. Banks, A. Crossley and R. G. Compton, *ChemPhysChem*, 2006, **7**, 1337-1344.
28 P. Chen and R. L. McCreery, *Anal. Chem.*, 1996, **68**, 3958-3965.
29 R. S. Nicholson, *Anal. Chem.*, 1965, **37**, 1351-1355.
30 C. Barbero, J. J. Silber and L. Sereno, *J. Electroanal. Chem.*, 1988, **248**, 321-340.
31 J. G. S. Moo, A. Ambrosi, A. Bonanni and M. Pumera, *Chem. Asian J.*, 2012, **7**, 759-770.
32 W. J. Blaedel and R. C. Engstrom, *Anal. Chem.*, 1978, **50**, 476-479.
33 A. Bonanni, A. Ambrosi and M. Pumera, *Chem. Eur. J.*, 2012, **18**, 4541-4548.
34 Y. Li, M. Liu, C. Xiang, Q. Xie and S. Yao, *Thin Solid Films*, 2006, **497**, 270-278.
35 T. Kiss and A. Gergely, *Inorg. Chim. Acta*, 1979, **36**, 31-36.